Formation of High-Quality Self-Assembled Monolayers of Conjugated Dithiols on Gold: Base Matters

Hennie Valkenier,[†,‡] Everardus H. Huisman,[‡,||] Paul A. van Hal,[§] Dago M. de Leeuw,[‡,§] Ryan C. Chiechi,*,[†,‡] and Jan C. Hummelen*,[†,‡]

[†]Stratingh Institute for Chemistry and [‡]Zernike Institute for Advanced Materials, University of Groningen, Nijenborgh 4, 9747 AG Groningen, The Netherlands

[§]Philips Research Laboratories, High Tech Campus 4, 5656 AE Eindhoven, The Netherlands

Ⓢ *Supporting Information*

ABSTRACT: This Article reports a systematic study on the formation of self-assembled monolayers (SAMs) of conjugated molecules for molecular electronic (ME) devices. We monitored the deprotection reaction of acetyl protected dithiols of oligophenylene ethynylenes (OPEs) in solution using two different bases and studied the quality of the resulting SAMs on gold. We found that the optimal conditions to reproducibly form dense, high-quality monolayers are 9−15% triethylamine (Et_3N) in THF. The deprotection base tetrabutylammonium hydroxide (Bu_4NOH) leads to less dense SAMs and the incorporation of Bu_4N into the monolayer. Furthermore, our results show the importance of the equilibrium concentrations of (di)thiolate in solution on the quality of the SAM. To demonstrate the relevance of these results for molecular electronics applications, large-area molecular junctions were fabricated using no base, Et_3N, and Bu_4NOH. The magnitude of the current-densities in these devices is highly dependent on the base. A value of $\beta = 0.15$ Å^{-1} for the exponential decay of the current-density of OPEs of varying length formed using Et_3N was obtained.
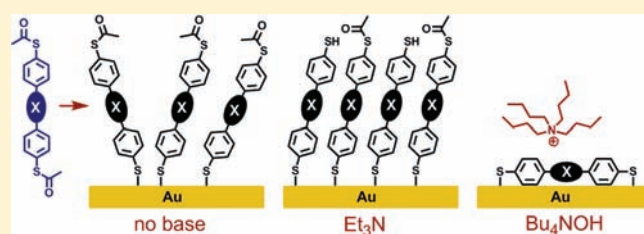
■ INTRODUCTION

This Article describes the influences of the base on the quality and density of self-assembled monolayers (SAMs) of thiolates of oligo(phenylene ethynylenes) (OPEs) and terphenylenes for molecular-electronic (ME) applications from the in situ deprotection of acetyl thioesters (Figure 1). We studied the influence of two commonly used bases, tetrabutylammonium hydroxide (Bu_4NOH) and triethylamine (Et_3N), in THF by forming SAMs comprising oligo(phenylene ethynylene)dithiolates, monothiolates, and terphenyldithiolates on gold and varying the concentrations of the base and the thioester. We followed the deprotection process using UV−vis and ^{1}H NMR spectroscopy to identify and differentiate the species that are present during the self-assembly process and measured the thickness, composition, and quality of the resulting SAMs using ellipsometry, XPS, and electrochemical measurements, respectively. We found that high concentrations of Et_3N (9−15% v/v) in THF reproducibly gave the best agreement between predicted and measured thickness of the SAMs, while the thickness of the SAMs that were formed using Bu_4NOH varied considerably with concentration. The SAMs formed using Et_3N were also more densely packed than those formed from Bu_4NOH. These findings highlight the importance of careful, optimized experimental procedures and an understanding of the underlying mechanisms when forming SAMs of OPEs and phenylenes, particularly when these SAMs will be used as the basis for further studies in ME devices and measurements.[1−4] We demonstrate the high quality and reproducibility of these SAMS in electrochemical analyses and by fabricating large-area molecular junctions (LAMJs)[5] of a series of OPEs using the optimized methods presented here and measuring the dependence of the tunneling-current on the thickness of the resulting SAMs.

Conjugated molecules and, in particular, OPEs and phenylenes are a critical component of ME devices because they enable the control of the tunneling of electrons by synthetic chemistry. In these devices, the SAM is used to define the smallest dimension of the device (i.e., the tunnel-junction between the electrodes), while the lateral dimension can be relatively large (up to hundreds of micrometers). Therefore, the reliable, reproducible formation of densely packed, high-quality SAMs over large areas is absolutely required. This is in contrast to the formation of junctions of single molecules, for example, mechanically controllable break junctions and STM break junctions, where lower coverages are often preferred over densely packed SAMs. These issues are less evident for SAMs of alkanethiolates because of the well-known insensitivity of the quality of these SAMs to the conditions of formation.[6] However, unlike simple alkanes, conjugated molecules are not sufficiently air-stable as free thiols to form SAMs and therefore must be protected, typically as acetyl thioesters, because they are stable and easy to prepare. Thus, SAMs are routinely formed by cleaving the
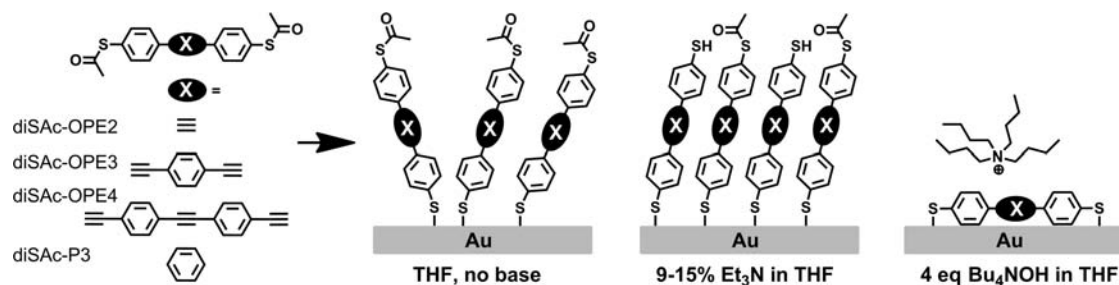
Figure 1. A schematic of the self-assembled monolayers on gold that are formed from solutions of OPE and terphenyl dithioesters in THF: without base, a SAM of about 70% of the maximum density is formed, with 9−15% (v/v) Et$_3$N, densely packed SAMs are formed, and with 4 equiv of Bu$_4$NOH, the molecules lay flat on the surface, and Bu$_4$N$^+$ is incorporated in the SAM.

acetyl thioesters with a base, generating the free thiolate in situ. The exact procedure, base, concentrations of thioester and base, immersion times, etc., of this deprotection, however, varies somewhat arbitrarily between laboratories and studies. This lack of reproducible protocols and adequate characterization hinders the meaningful interpretation of electronic measurements on devices containing these conjugated SAMs.

The first study on the formation of SAMs from conjugated thiols, acetyl thioesters, and deprotected thioacetates was reported by Tour et al.[7] They demonstrated that the ellipsometric thicknesses of SAMs of conjugated monothiols grown from THF reach the expected value within 24 h, while dithiols form multilayers.[7,8] If the dithiols are first protected as acetyl thioesters, the resulting SAMs do not form multilayers, but are thinner than expected.[7,9,10] When the acetyl thioesters are hydrolyzed in situ with NH$_4$OH, Tour et al. also observe the formation of multilayers.[7] Despite this observation, over the past 15 years, this paper[7] has been frequently and incorrectly cited as evidence of the formation of high-quality SAMs of conjugated dithiols formed from the in situ deprotection of acetyl thioesters with NH$_4$OH. Some studies report reasonable thicknesses using NH$_4$OH,[11−15] while others report thicknesses that are higher than the calculated value,[11,16,17] and impurities attributed to the NH$_4$OH are reported.[18] The problem with NH$_4$OH is that it is only effective in polar, protic solvents (usually ethanol, which is also commonly used with alkanethiols). Conjugated, rigid-rod molecules such as OPEs and phenylenes, however, are not compatible with protic solvents; thus SAMs of these molecules are typically formed from aprotic solvents (usually THF). This incompatibility makes it impossible to control the concentration of NH$_4$OH (which is 30% aqueous NH$_3$) because it is lost as NH$_3$, particularly while sparging with an inert gas. Despite this fact, NH$_4$OH is commonly used in aprotic solvents, which can lead to irreproducible, low-quality, loosely packed SAMs. Using NaOH as deprotecting agent causes similar problems[19] and damages the metal substrate.[20]

Tour et al. used Et$_3$N to favor the thiolate form of thiophenethiol over the dimeric form,[7,21] but not to deprotect thioesters. Other studies use Et$_3$N to form thiols from nonthioester precursors.[22,23] Shaporenko et al. compared SAMs formed from biphenyldiacetylthiolate using "appropriate amounts" of Et$_3$N to those using NH$_4$OH and found that the former produced SAMs that were more densely packed.[16] There are other studies on the deprotection of conjugated OPE monothioacetates;[24−26] however, they focus on other aspects (e.g., reactions between the deprotecting agent and other functional groups) and do not observe the difficulties that are inherent to dithiols. We chose to study Bu$_4$NOH as a nonvolatile analogue of NH$_4$OH because it

is commonly used to deprotect conjugated dithioacetates in situ for ME measurements in mechanically controllable break-junctions[27−30] and STM break-junctions.[31] We chose Et$_3$N because of the promising results of Shaporenko et al.,[16] and the need for high-quality, densely packed SAMs of conjugated molecules for ME devices using, for example, μ-contact printing,[32−34] conjugated polymers,[5,35] Hg,[36−38] eutectic GaIn,[39,40] and CP-AFM[41−44] to contact the SAM.[45−48]

■ EXPERIMENTAL SECTION

Chemicals and Synthesis. diSAc−OPE3 and diSAc−P3 were synthesized according to literature procedures.[49,11] We recently reported the synthesis of compounds diSAc−OPE2 and diSAc−OPE4 elsewhere.[50] The synthesis of SAc−OPE2 and SAc−OPE3 is described in the Supporting Information.

Benzenedithiol was purchased from TCI (>95%) and benzene-(mono)thiol from Aldrich (>99%). Tetrahydrofuran (THF) was dried by percolation over columns of aluminum oxide and R3-11-supported Cu-based oxygen scavengers, degassed, and stored under nitrogen. THF-d$_8$ was dried and degassed a prior to use. Triethylamine (Et$_3$N) was distilled over KOH under nitrogen or purchased from Fisher (HPLC grade) and degassed. Tetrabutylammonium hydroxide 30-hydrate (Bu$_4$NOH) was purchased from Sigma-Aldrich and stored under nitrogen.

Substrates. 150 nm Au was thermally evaporated onto freshly cleaved mica after heating the mica for 16 h at 375 °C in vacuo. The samples were heated for one more hour after the deposition, then gradually cooled to room temperature, taken from the vacuum chamber, cut into pieces, and transferred into the glovebox for immersion in a thiolate solution. For the electrochemical measurements, commercial 1 in. glass disks coated with 200 nm Au were used (Ssens BV, Hengelo). These were cleaned with acidic piranha (1 part 30% H$_2$O$_2$ added to 3 parts 98% H$_2$SO$_4$; Caution: Dangerous!), rinsed with water and ethanol, and dried with a nitrogen flow prior to use.

Preparation of Solutions and Formation of SAMs. All solutions and SAMs were prepared inside a glovebox filled with nitrogen (<5 ppm O$_2$). THF was used as solvent in all reported experiments. Solutions of diSAc−OPE4 were stirred and heated to 50 °C and filtered through a 1 μm PTFE syringe filter by gravity prior to monolayer growth. After the given immersion time, samples were taken from solution and immersed three times in vials with clean THF, after which the samples were dried in the glovebox or with flowing nitrogen.

UV−Vis Absorption. UV−vis absorption spectra were measured on a Perkin-Elmer Lambda 900 spectrometer in a 1 mm quartz cuvette with Teflon stopper, typically in 30−60 min after preparation of the solution, unless indicated otherwise.

^{1}H NMR. ^{1}H NMR measurements were recorded on a Varian AMX400 (400 MHz) or Varian unity plus (500 MHz) NMR

spectrometer in THF-d_8. J. Young NMR tubes were used to keep the solutions under nitrogen during the measurement. Spectra were referenced to the solvent signal (3.60 ppm for THF-d_8).

Ellipsometry. Ellipsometry measurements were performed using a V-Vase from J. A. Woollam Co., Inc. in air. Measurements were acquired from 300 to 800 nm with an interval of 10 nm at 65°, 70°, and 75° angles of incidence. For every set of experiments, a fresh gold-on-mica sample was measured at three or four different spots. The data from these measurements were merged, and the optical constants were fitted. For every SAM, three spots were measured, and the thickness of a cauchy layer ($n = 1.55$, $k = 0$ at all λ) on top of the gold layer was fitted. The thicknesses are reported as the average of the three spots with the standard deviation as the error bar.

XPS. XPS measurements were performed on a X-PROBE Surface Science Laboratories photoelectron spectrometer with an Al Kα X-ray source (1486.6 eV) and a takeoff angle of 37°. We accumulated 20 scans for S2p, 10 for C1s, 10 for O1s, 15 for N1s, and 5 for Au4f. All reported data are averaged over four different spots per sample. WinSpec[51] was used to fit the recorded data with a background and minimum number of mixed Gaussian−Lorentzian singlets (C1s, N1s, O1s) or doublets (Au4f; $\Delta = 3.67$ eV, S2p; $\Delta = 1.18$ eV) with a width of 1.21 eV. For details on the estimation of the thickness of the SAMs based on XPS results, see the Supporting Information.

Electrochemistry. Electrochemical measurements were performed with an Autolab PGSTAT10 in a three-electrode liquid cell, with the gold working electrode mounted at the bottom of the cell (area = 0.44 cm^2), a platinum disk counter electrode, and a Hg/HgSO$_4$ reference electrode ($+0.64$ V vs SHE). Capacitance measurements were performed electrochemically by cyclic voltammetry (-0.1 to -0.4 V) in 0.1 M K$_2$SO$_4$ in water at 50, 100, 200, 300, and 500 mV/s. The average of the positive and negative current at -0.25 V was plotted versus the scan speed. The slope of this plot gives the electrochemical capacitance value of the SAM (see Figure S13). The packing density of the SAMs was studied in a solution of 50 μM FeK$_3$(CN)$_6$ and 50 μM FeK$_4$(CN)$_6$ as redox couple in 0.1 M K$_2$SO$_4$ in water by cyclic voltammetry (0.3 to -0.6 V) at 100 mV/s.

Large-Area Molecular Junctions. The large-area molecular junctions were fabricated and measured as described by van Hal et al.,[52] using MA1407 photoresist. SAMs were grown by immersion in 0.5 mM solutions in THF with Et$_3$N (for the acetyl protected compounds) for 2 days. The SAM of diSAc−OPE4 was grown from a filtered 0.1 mM solution.

■ RESULTS AND DISCUSSION

Nomenclature. We abbreviate acetyl as "Ac" and thiolates as "S" (i.e., we omit the minus sign of S$^-$) such that SAc is the protected acetyl−thioester. We refer to monoacetyl-protected monothiols with the prefix "SAc" and diacetyl−protected dithiols with the prefix "diSAc."

We define high-quality SAMs as being free of pinholes, as determined by electrochemical measurements. We define densely packed as a SAM in which the thickness measured by ellipsometry is reproducibly within 80−100% of the maximum theoretical thickness (i.e., the length of the molecule +2.3 Å for the S−Au bond). We use the term cyclic voltammetry (CV) only to refer to three-electrode electrochemical measurements in solution.

Forming SAMs from Thioesters of OPEs. When generating thiolates from thioesters to form monolayers, both the mechanisms of the deprotection of acetyl thioesters and the formation of SAMs must be considered. A mixture of thioesters, in the presence of a thiolate (i.e., R−S, not R−SH), will metathesize
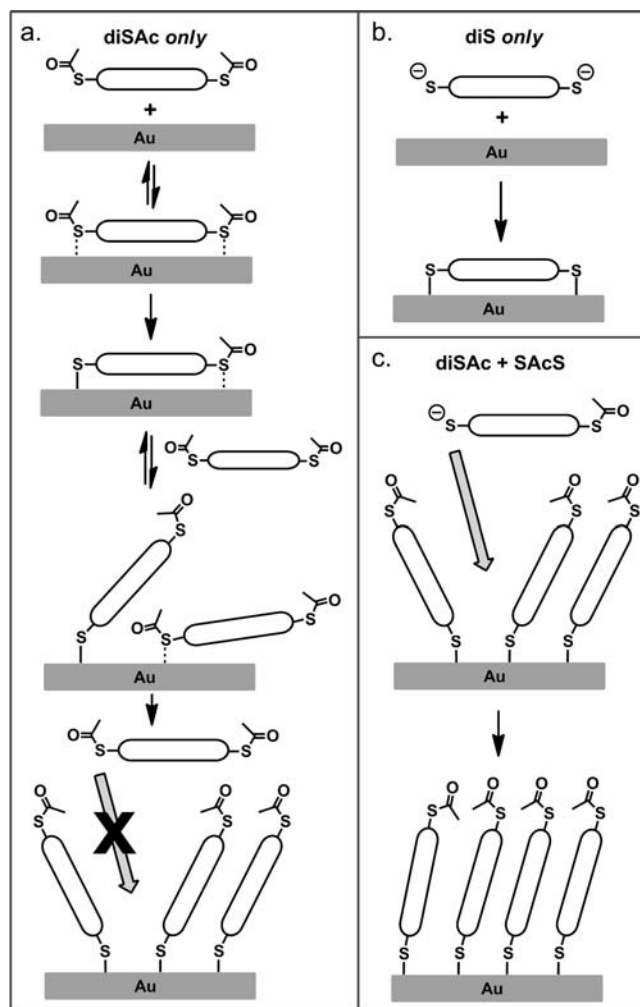
Figure 2. A schematic of the kinetics of the formation of self-assembled monolayers on gold from solutions of (a) diSAc only, incomplete coverage due to weak association with the surface and slow incorporation into the monolayer; (b) diS only, strong association with the gold surface hinders self-assembly; polymeric disulfides form readily and precipitate; and (c) diSAc plus SAcS, self-assembly occurs similarly to diSAc-only except SAcS incorporates readily, resulting in a densely packed monolayer.

to form equilibrium mixtures that reflect the initial concentration of thiolate and the relative stabilities of the various thiolates and thioesters.[53,54] For example, introducing R^1−S to a solution of R^2−SAc forms a mixture of R^1−SAc, R^1−S, R^2−SAc, and R^2−S (see Figure S2). Because this equilibration occurs on a microsecond time scale in solution and the formation of a SAM occurs at the interface between the solution and the substrate on a minute time scale, the solution from which the SAM forms is highly dependent on how much thiolate is generated from the deprotecting agent. (The removal of thiolate by the growing SAM has a negligible impact at the concentrations typically used.) This means that, in the case of a dithiol, there will be a competition between the diSAc−OPE, SAc−OPE−S, and diS−OPE, each of which interacts differently with the substrate (see Figure 2).

The formation of a SAM occurs in three basic steps: (i) association between molecules and substrate where the molecules lie down on the surface, (ii) reorganization of these
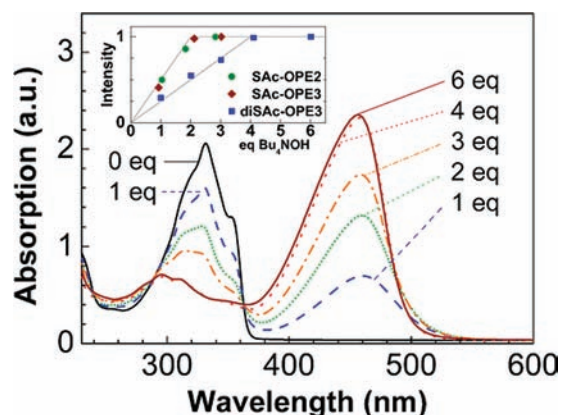
Figure 3. UV−vis absorption spectra of 0.3 mM diSAc−OPE3 in THF with 0 equiv (black, −), 1 equiv (blue, − − −), 2 equiv (green, · · ·), 3 equiv (orange, − · − · −), 4 equiv (red, - - -), and 6 equiv Bu$_4$NOH (dark red, −), showing the conversion of thioacetate into free thiolate. The inset is a plot of the normalized intensity of the growing absorption peak as function of the number of equivalents of Bu$_4$NOH added for molecules diSAc−OPE3, SAc−OPE3, and SAc−OPE2: diSAc−OPE3 reacts with 4 equiv of base, whereas SAc−OPE2 and SAc−OPE3 react with 2 equiv of base.

molecules into islands of loosely packed standing molecules (observed as striped phases for alkanethiolates), and (iii) growth of these islands into a densely packed monolayer.[55] The transition from lying-down to standing up is driven by the strength of the Au−thiolate bond and can only occur if the association with surface is weak enough to be reversible on the time scale of the experiment (dotted lines in Figure 2a). Likewise, the growth of the domains of standing molecules can only occur only if each step is reversible and the densely packed monolayer is the most thermodynamically stable.[56] Thiolates associate much more strongly than thiols or thioesters, but Au cleaves thioesters (and thiols) to form Au−thiolates. The resulting Au-bound thiolates dissociate as Au complexes; thus they do not participate in further thioester metathesis (i.e., the reaction of Au with SAc−OPE does not produce any free S−OPE).

SAMs of diS−OPE (Figure 2b) are arrested at step i: interactions between the Au surface and the π-electrons in combination with two highly reactive thiolates drives the equilibrium between the standing-up phase and lying-down too far toward the lying-down phase for a SAM to form. By contrast, in a solution composed mainly of diSAc−OPE3 and/or SAc−OPE3−S, the equilibrium is pushed toward the standing-up phase by the poor interaction of the SAc groups with the Au surface (and the favorable packing of these groups in the SAM). Although diSAc−OPE tends to form standing-up SAMs (Figure 2a), the thioacetates are too bulky to fill the last vacancies in the SAM. This can be solved by the presence of SAc−OPE−S in the solution (Figure 2c), even in small quantities.[57]

Deprotection Using Bu$_4$NOH. We followed the deprotection reaction by recording UV−vis spectra of 0.3 mM diSAc−OPE3 in THF during the addition of 6 equiv (relative to the number of diSAc−molecules; i.e., 3 equiv of per SAc) of Bu$_4$NOH. The solutions changed from colorless to bright orange to yellow as the free thiolates formed (Figure 3).

During the addition of the first 2 equiv of Bu$_4$NOH, a new absorption peak appeared at 460 nm, which we ascribe to delocalized thiolates. This peak increased in intensity and gradually shifted to 458 nm during the addition of equivalents
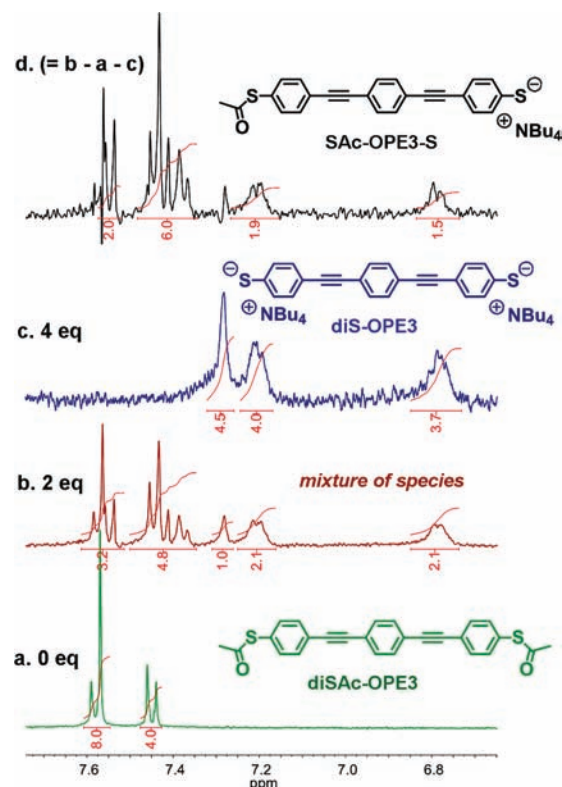
Figure 4. ^{1}H NMR spectra from 7.7 to 6.7 ppm, of 0.3 mM diSAc−OPE3 in THF-d_8 (spectrum a), with addition of 2 equiv of Bu$_4$NOH (spectrum b), with addition of 4 equiv of Bu$_4$NOH (spectrum c), and the spectrum of b with a and c subtracted (spectrum d), which shows that in addition to diSAc−OPE3 and diS−OPE3, the asymmetric SAc−OPE3−S persists in the solution with 2 equiv of Bu$_4$NOH.

three and four and remained constant through equivalents five and six, indicating that 2 equiv of Bu$_4$NOH reacts with each SAc in diSAc−OPE3. We repeated this experiment with SAc−OPE3, SAc−OPE2, diSAc−OPE2, and diSAc−P3 and observed the same result; 2 equiv of Bu$_4$NOH remove one Ac (Figures S4 and S5). The first equivalent hydrolyzes the Ac through simple addition/elimination, and the second deprotonates the acetic acid that is formed in the first step (Figure S1). The linear dependence of the increase in intensity at 458 nm (Figure 3, inset) and commensurate decrease at 331 nm with increasing Bu$_4$NOH, and the semi-isosbestic point at 363 nm, indicate that there are no intermediate chromophores between the SAc and S compounds. There must, however, be a monodeprotected intermediate (SAc−OPE3−S).

To probe for this intermediate, we prepared four solutions of 0.3 mM diSAc−OPE3 in THF-d_8 with 0, 1/2, 2, and 4 equiv of Bu$_4$NOH and examined them using ^{1}H NMR spectroscopy (Figure 4). The spectrum of the solution containing 4 equiv of Bu$_4$NOH consisted of three peaks (Figure 4c) that are shifted upfield relative to diSAc−OPE3 (Figure 4a), which we ascribe to diS−OPE3.[58] Assuming that the solution containing 2 equiv of Bu$_4$NOH (Figure 4b) comprised a mixture of diSAc−OPE3, SAc−OPE3−S, and diS−OPE3, we subtracted these two spectra (a and c) from (b) to isolate the spectrum of SAc−OPE3−S (Figure 4d). We integrated the peaks in the aromatic region (6.7−7.7 ppm) to determine that the solution with 2 equiv of Bu$_4$NOH comprised 22% diSAc−OPE3, 56% SAc−OPE3−S, and 22% diS−OPE3, a ratio of 1:2:1. We repeated this analysis
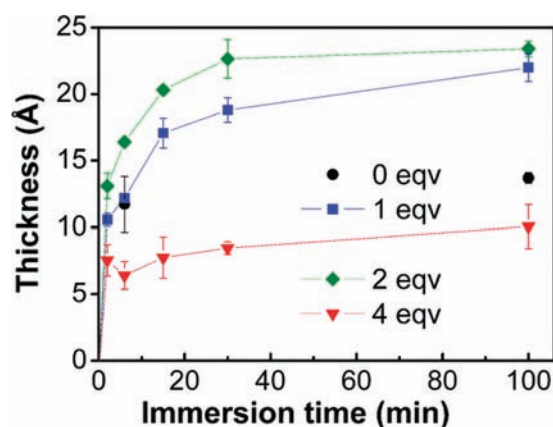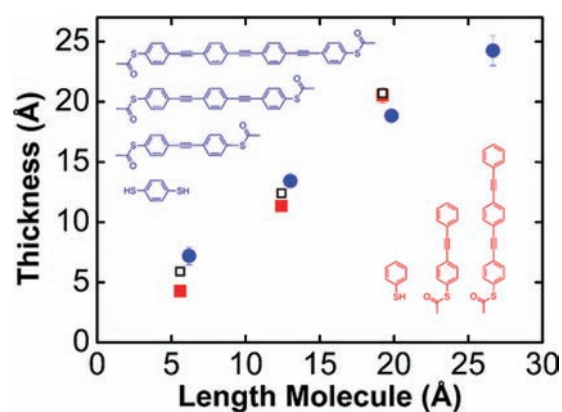
Figure 5. Ellipsometric thicknesses (Å) of the SAMs formed from 0.3 mM diSAc—OPE3 as function of the immersion time, with 0 equiv (●), 1 equiv (blue ■), 2 equiv (green ◆), and 4 equiv of Bu$_4$NOH (red ▼). SAMs with 1 and 2 equiv give reasonable thicknesses in about 1 h.

Figure 6. A plot showing a linear increase of the thicknesses of SAMs of OPE—dithiols (blue structures, upper-left) and OPE monothiols (red structures, lower-right), formed after 2 days immersion time in solutions with 9—15% Et$_3$N, with their length. SAMs of benzenedithiol, diSAc—OPE2, diSAc—OPE3, and diSAc—OPE4 were measured by ellipsometry (blue ●), and those of benzene monothiol, SAc—OPE2, and SAc—OPE3 were measured by ellipsometry (red ■) and XPS (black □).

and determined that the ratio of the solution containing 1/2 equiv of Bu$_4$NOH was 3:1:0.[59] This means that the three species coexist as a statistical mixture in solution (due to the metathesis of the thioesters), in a ratio determined by the amount of Bu$_4$NOH and with no preference for the formation of a particular species. These observations are in agreement with the UV—vis data, which show a single absorption growing in intensity with the addition of Bu$_4$NOH, meaning that the absorptions of the thiolates of SAc—OPE3—S and diS—OPE3 are nearly identical.

Forming SAMs of OPEs Using Bu$_4$NOH. We examined the influence of the concentration of Bu$_4$NOH on the formation of SAMs of OPEs by immersing Au substrates in 0.3 mM solutions of diSAc—OPE3 and either 0, 1, 2, or 4 equiv of Bu$_4$NOH and measuring the thicknesses of the resulting SAMs using ellipsometry (Figure 5). These values are based on the assumptions that the index of refraction of a monolayer of conjugated molecules is 1.55,[7,11] and that the absorption of the SAMs can be neglected; they are accurate to ±2 Å. Lower values indicate a SAM that is less densely packed, but we cannot determine the cause (i.e., the structure of the SAM) using only ellipsometry.[9]

Within 2 h, the thicknesses measured for the SAMs formed using 1 or 2 equiv of Bu$_4$NOH matched the predicted value (24.9 Å),[60] indicating the presence of a densely packed monolayer composed of S—OPE3—SAc and S—OPE3—S. The thicknesses measured for SAMs that were immersed for longer than 2 h were irreproducible and usually larger than the predicted value, which may indicate the formation of multilayers as Tour et al. reported for NH$_4$OH.[7] Regardless of the cause, this observation means that SAMs formed from solutions with Bu$_4$NOH lack the reproducibility required for ME devices.

In the absence of Bu$_4$NOH (0 equiv), we measured thicknesses of 14 Å after 100 min and 15 Å after 24 h, which is about 70% of the predicted value. This result indicates that, as expected, diSAc—OPE3 can form monolayers without in situ deprotection, but that these SAMs are not densely packed (Figure 2a). Using 4 equiv of Bu$_4$NOH, we measured a thicknesses of only 10 Å, meaning that diS—OPE3 forms worse monolayers than does diSAc—OPE3. Upon immersing the Au substrates in the solutions with 4 equiv of Bu$_4$NOH, an orange precipitate formed that we ascribe to the formation of insoluble disulfide precipitates. We observed this precipitate in the NMR tube after exposure to

oxygen (Figure S8). It is unlikely, however, that micrometer-scale precipitates influence the formation of the SAMs, which happens on molecular length scale.

To broaden the scope of our results, we repeated the UV—vis and ellipsometry experiments for diSAc—P3 (deprotected with Bu$_4$NOH) and found the same results as for diSAc—OPE3 (see Figures S6 and 7). Furthermore, these experiments allowed us to relate our results to previous studies of Krapchetov et al.[61] on diSAc—P3 deprotected with NH$_4$OH (see the Supporting Information). The published data support our hypothesis, which is depicted in Figure 2.

Forming SAMs of OPEs Using Et$_3$N. To the best of our knowledge, the only report on using Et$_3$N to form SAMs from acetyl thioesters of conjugated dithiols is from Shaporenko et al.[16,62] They observed densely packed SAMs, but did not describe the exact conditions used. This may be because the quality of SAMs of OPEs formed using Et$_3$N is much less sensitive to an excess of base than, for example, SAMs formed using Bu$_4$NOH. We investigated the effects of the concentration of Et$_3$N on the formation of SAMs from diSAc—OPE2, diSAc—OPE3, diSAc—OPE4, SAc—OPE2, and SAc—OPE3 by immersing Au substrates in solutions of different concentrations of Et$_3$N and 0.5 mM of each of these compounds in THF (except diSAc—OPE4, which saturated above 0.1 mM)[63] and measuring the thicknesses of the resulting SAMs by ellipsometry (Table S1). Using 3% (v/v) Et$_3$N with diSAc—OPE3, we observed reasonable thicknesses, but SAMs of diSAc—OPE4 were too thin. For 9—15% (v/v) Et$_3$N, we measured a linear increase in the thicknesses of the SAMs with increasing length of molecules (Figure 6), in contrast to SAMs grown from solutions with Bu$_4$NOH or without base (Figure S5).

We followed the deprotection reaction using Et$_3$N by acquiring UV—vis spectra for a 0.3 mM solution of diSAc—OPE3 in a 12% solution of Et$_3$N in THF after 5 min, 24 h, and 48 h (Figure S9). The spectrum did not change appreciably, and there were no peaks at 458 or 460 nm, indicating a lack of thiolate in solution. Unlike Bu$_4$NOH, Et$_3$N is a hindered, non-nucleophilic base, and therefore the mechanism of the deprotection probably proceeds through the generation of a ketene. Ketenes are normally

Table 1. Composition of the SAMs: X-ray Photoelectron Spectroscopy Measurements

	integrated intensities[a]							normalized intensities
conditions	Au4f	C1s C_xH_y	C1s C=O	S2p S—Au	S2p S—R	O1s	N1s	C1s per OPE C-atom[b]
0.5 mM diSAc—OPE3 in THF	83.98 eV	283—287 eV	288 eV	162 eV	164 eV	532 eV	403 eV	283—287 eV
no base, 70 h	65 020	977	39	30	39	43		43
15% Et$_3$N, 46 h	54 227	1229	28	33	72	40		55
3 mM Bu$_4$NOH, 40 min	60 156	633		5			17	17
(1) no base, 70 h, (2) 20 mM Bu$_4$NOH, 80 s[c]	39 315	860		29	12	15	25	21
(1) 15% Et$_3$N, 49 h, (2) 20 mM Bu$_4$NOH, 7 min[c]	29 010	696		20	12	20	20	17

[a] These areas are divided by the sensitivity factor: 1 for C1s, 1.79 for S2p, 2.49 for O1s, and 1.68 for N1s. For Au4f, the total area is reported (not divided by a sensitivity factor). [b] The total area of the C_xH_y C1s signal is divided by the number of C-atoms in the OPE core. We correct for the presence of other C-atoms: (1) from the acetyl group, by assuming that the intensity of CH$_3$ is the same as C=O, and (2) from Bu$_4$N$^+$, by assuming that the intensity of the N1s signal only comes from Bu$_4$N$^+$, and that the 16 C atoms of Bu$_4$N$^+$ each contribute with the same intensity to the C1s signal. [c] SAMs were prepared in two steps: the first step is the immersion in OPE-solution, and the second step is the treatment with a 20 mM Bu$_4$NOH solution in THF (without OPE molecules).

generated by treating acid chlorides/bromides with a non-nucleophilic base[64,65] (e.g., acetyl chloride and Et$_3$N), which abstracts an α-proton and eliminates chloride/bromide, reforming the carbonyl with a cumulative double bond (Figure S3). While thioesters normally do not form ketenes, here the thiolate leaving-group is sufficiently delocalized to make it stable enough to form a small amount of ketene (and the commensurate OPE thiolate). Taking into account the fact that (loosely packed) SAMs can form directly from acetyl thioesters, we propose the following mechanism for the formation of SAMs from diSAc—OPE3 and Et$_3$N: diSAc—OPE3 adsorbs to the Au substrate where it is slowly converted to SAc—OPE3—S—Au, eventually forming a very sparse monolayer comprising small domains of standing-up phases, disordered phases, and lying-down phases (which we observe as a smaller ellipsometric thickness than the predicted value). The slow reaction between Et$_3$N and diSAc—OPE3 in solution produces an amount of SAc—OPE3—S that is small enough that effectively no diS—OPE3 is formed. This small amount is below the detection limit of our UV—vis experiments. The SAc—OPE3—S that does form, however, associates strongly with the Au substrate, displacing adsorbed diSAc—OPE3 and incorporating itself into the standing-up phase, forming a densely packed SAM as drawn in Figure 2c that we observe as an ellipsometric thickness that equals the predicted value. These are the ideal conditions for self-assembly because each step is highly reversible: diSAc—OPE3 forms a weakly adsorbed lying-down phase, and the low concentration of SAc-OPE3-S prevents driving the equilibrium too far toward the (disordered) chemisorbed state. Over the course of 24—48 h, this process forms a high-quality, densely packed monolayer.

Determining the Composition of the SAMs. We used X-ray photoelectron spectroscopy (XPS) to determine the composition of SAMs formed from benzenethiol, SAc—OPE2, and SAc—OPE3 (see Figure S11). We found only one S2p doublet at 162 eV for all of the SAMs formed from monothiols, indicating that all of the sulfur atoms in the SAM are bound to Au. From the same data, we estimated the thicknesses of the SAM by determining the ratio of the areas of the peaks corresponding to C1s and Au4f and found good agreement with those determined by ellipsometry (Figure 6, see Table S2 for more details). We varied the conditions of the formation of the SAMs from diSAc—OPE3 to determine the influence of the ratios of diSAc—OPE3, SAc—
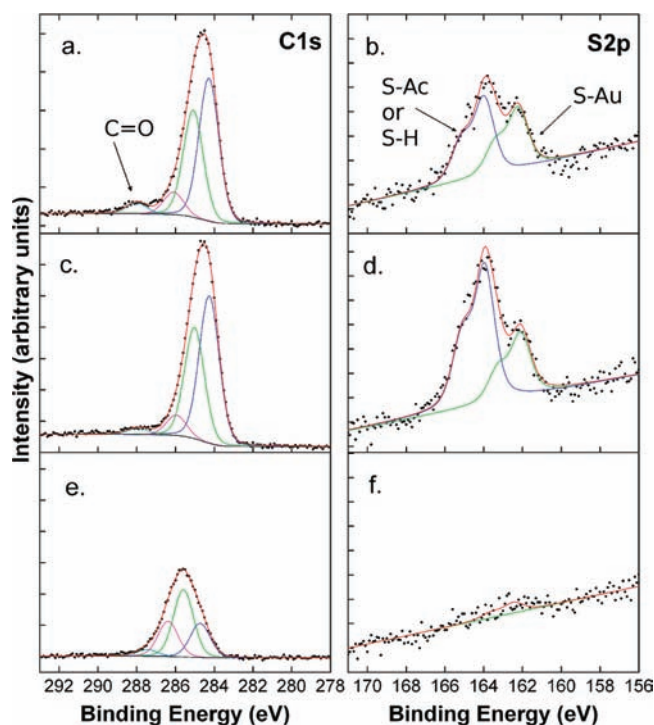
Figure 7. C1s (a,c,e) and S2p (b,d,f) XPS signals for SAMs from diSAc—OPE3 without base (a and b), with 15% Et$_3$N (c and d), and with 6 equiv of Bu$_4$NOH (e and f). Fits are shown as colored lines. In the SAM grown without base, acetyl groups are clearly present. Less acetyl groups are present in SAM grown with Et$_3$N. Both SAMs clearly contain both S atoms bound to gold and S atoms that are not bound to gold. There is no evidence for S atoms that are not bound to Au in the SAM grown using Bu$_4$NOH.

OPE3—S, and diS—OPE3 that are present in solution. We measured SAMs formed from three solutions: 0.5 mM diSAc-OPE3 and (i) no base, (ii) 15% Et$_3$N, and (iii) 6 equiv of Bu$_4$NOH (Table 1 and Figure S12). We chose these three conditions because (i) serves as a control and (ii) and (iii) are the boundary conditions for the formation of thiolate: no dithiolate and no monothiolate, respectively. The thicknesses measured by XPS were 13.1 Å for no base, 17.5 Å for 15% Et$_3$N,
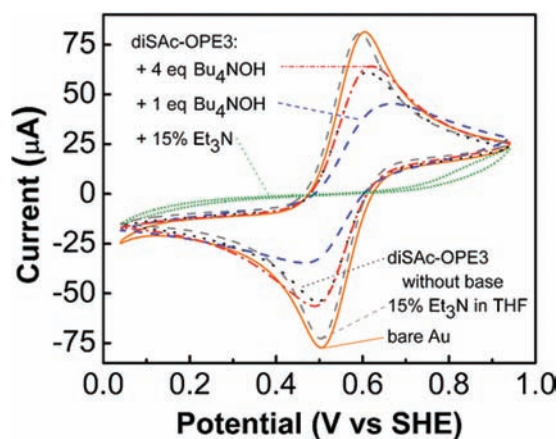
Figure 8. Cyclic voltammograms of 50 μM FeK$_3$(CN)$_6$ and 50 μM FeK$_4$(CN)$_6$ as a redox couple in 0.1 M K$_2$SO$_4$ in water at 100 mV/s with Hg/HgSO$_4$ as reference electrode, a Pt disk counter electrode, and gold disk working electrode (0.44 cm^2) with diSAc−OPE3 and 4 equiv of Bu$_4$NOH (red, − · − · −), diSAc−OPE3 and 1 equiv of Bu$_4$NOH (blue, − − −), diSAc−OPE3 and 15% Et$_3$N (green, · · ·), diSAc−OPE3 without base (black, - - -), bare gold (orange, −), and gold immersed in 15% Et$_3$N in THF without OPE (gray, − − −). Only the SAM of diSAc−OPE3 formed using 15% Et$_3$N completely blocks the Fe^{2+}/Fe^{3+} redox signal, indicating a densely packed SAM that is free of pinholes.

and 9.8 Å for 6 equiv of Bu$_4$NOH; we observed the same trend by ellipsometry (see notes of Table S2 for more details).

The XPS spectra of the SAM formed without base shows two sulfur peaks, one bound to Au (162 eV) and one unbound sulfur atom (164 eV) as shown in Figure 7. The integral of the peak corresponding to the sulfur atoms that are bound to gold is smaller than that for the unbound sulfur atoms because the signal for the buried sulfur atoms is attenuated by the SAM. The integrals of the peaks corresponding to the carbon (C1s, 288 eV) and oxygen (O1s, 532 eV) of the carbonyl are equal to that of unbound sulfur (Table 1). We did not observe any other sulfur or oxygen peaks; thus we conclude that the SAM is composed of SAc−OPE3−S bound to Au. The SAM formed using 15% Et$_3$N again shows two unequal sulfur peaks (162 and 164 eV), but the peak for S−Au was significantly smaller. This increased attenuation is again due to the increase in the density of the SAM formed using 15% Et$_3$N as compared to that formed without base. The integral of the peak corresponding to the carbonyl carbon (288 eV) is 70% of that of the oxygen (532 eV) and only 40% of that of unbound sulfur. Because there are only two sulfur peaks (and no peaks for S=O at 168 eV), it is unlikely that this excess oxygen is from oxides of sulfur. By comparing the integral of the peak corresponding to the carbonyl C1s to those of the carbon atoms in the OPE backbone and the signal of unbound sulfur, we conclude that 40−60% of the sulfur atoms that are not bound to Au are protected by acetyl groups. (The presence of free thiols may be causing the apparent increase in the amount of oxygen by inducing surreptitious, oxygen-rich compounds to adsorb to the surface.) By comparison, Shaporenko et al. estimated this value to be 10−20% for SAMs of diSAc−biphenyls.[16] We cannot exclude the presence of small amounts of additional molecules bonded to the surface of the SAM through disulfides from our XPS data because the S2p signal from disulfides cannot be distinguished from the S2p signals from unbound sulfur atoms (e.g., SH or SAc). However, we can exclude the formation of a

bilayer or multilayer because these would be apparent by ellipsometry. We could not identify any signals for nitrogen in the XPS data, indicating that none of the Et$_3$N was incorporated into the SAM.

The XPS data for SAMs formed using 6 equiv of Bu$_4$NOH show peaks for sulfur that are too small to draw any conclusions from (other than the fact that there is not much sulfur in the sample). No peaks corresponding to the carbon and oxygen of the carbonyl are visible, but there is a large nitrogen peak. This means that the SAMs formed from 6 equiv of Bu$_4$NOH (i.e., pure diS−OPE3) are not only significantly less dense than the other two samples, but also incorporate the counterion of the base (ratio OPE:Bu$_4$N$^+ \approx 1$). We treated the other two SAMs (no base and 15% Et$_3$N) with Bu$_4$NOH and measured them again. The resulting spectra show thicker SAMs with smaller signals for the carbonyl carbon and oxygen and the appearance of a nitrogen peak. We conclude that Bu$_4$NOH can be used to remove acetyl thioesters from the surface of a SAM, but that Bu$_4$N$^+$ ions are incorporated into the SAM (probably as counterions to the thiolates). Nevertheless, these results show that we cannot only determine the composition of head groups in SAMs from dithioacetates, but that we can control this composition.

Electrochemical Characterization of the SAMs. We measured the density of SAMs on Au discs formed from 0.3 to 0.5 mM diSAc−OPE3 in THF and (i) no base, (ii) 1 equiv of Bu$_4$NOH, (iii) 4 equiv of Bu$_4$NOH, and (iv) 15% (v/v) Et$_3$N using cyclic voltammetry (CV). We acquired CV data for these SAMs in a 0.1 mM aqueous K$_2$SO$_4$ electrolyte, containing a Fe^{2+}/Fe^{3+} redox couple, using the Au discs as the working electrode. We compared the redox waves to those for freshly cleaned Au (Figure 8). There were no redox waves present for SAMs formed using Et$_3$N, indicating that these SAMs were free of pinholes; that is, they are densely packed and high quality, covering 100% of the Au disk. Thus, with Et$_3$N we meet the most important requirement of SAMs for applications in molecular electronics: a densely packed and defect-free SAM reduces the formation of shorts.

The CV data for solutions comprising only Et$_3$N (no OPE) are identical to those for clean Au and have the largest current-density (J, 175 and 180 μA cm^{-2}, respectively). The second-largest J value is for SAMs formed using no base (132 μA cm^{-2}) and 4 equiv of Bu$_4$NOH (136 μA cm^{-2}). J is smaller for SAMs formed using 1 equiv of Bu$_4$NOH (91 μA cm^{-2}). These data agree with the data obtained using ellipsometry, and we can conclude that the thicknesses measured by ellipsometry that were lower than the predicted values correspond to SAMs that are less dense than 100% coverage.

Molecular-Electronic Devices from OPEs. To demonstrate the high quality and high reproducibility of SAMs grown with Et$_3$N on large areas, we determined the electrical properties of SAMs of benzenedithiol,[66] diSAc−OPE2, diSAc−OPE3, and diSAc−OPE4. This series allows a systematic study of both the capacitance and the current-density as a function of SAM thickness by using CV and LAMJs, respectively. For both methods, it is critical that the SAMs are densely packed and of high quality. In particular, CV measurements are sensitive to pinholes. Pinholes will expose the underlying Au substrate to the electrolyte, obfuscating the electrical properties of the SAM and increasing the measured capacitances.

We measured, by CV, the capacitance of SAMs formed using 15% (v/v) Et$_3$N in THF and 0.5 mM: (i) benzenedithiol,[66] (ii) diSAc−OPE2, (iii) diSAc−OPE3, (iv) diSAc−OPE4 (0.1 mM),
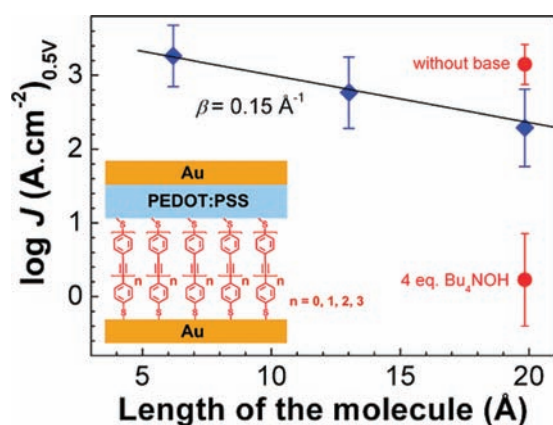
Figure 9. Average current-densities at 0.5 V for large-area molecular junction devices with diameters ranging from 5 to 50 μm. (The inset is a schematic (not to scale) of the architecture of the devices.) The blue "◆" show the average current-densities from two or three wafers each for optimized SAMs of benzenedithiol (0.5 mM in THF, without base), diSAc−OPE2 (0.5 mM in THF, 5−10% Et$_3$N added), and diSAc−OPE3 (0.5 mM in THF, 5−10% Et$_3$N added). The characteristic tunneling decay, β, from the linear fit (−) is 0.15 Å^{-1}. The red "●" show the average current-densities (one wafer each) of SAMs of diSAc−OPE3 grown under different conditions: 0.5 mM in THF without base gives current-densities that are higher than expected, and 0.3 mM in THF with 4 equiv of Bu$_4$NOH gives values that are much lower than expected (see labels); only SAMs formed using Et$_3$N lead to reproducible data between experiments.

and (v) Au disks immersed in 15% (v/v) Et$_3$N in THF without OPEs as a control (Figure S13). In these CV measurements in the absence of Fe^{2+}/Fe^{3+}, the SAM acts as the dielectric layer for a capacitor that is formed from the electrochemical double layer and the Au disk. We measured a decrease in capacitance for increasing thicknesses: 9.56, 6.53, 4.38, and 2.57 μF cm^{-2} for (v), (i), (ii), and (iii), respectively (as was found for SAMs of alkanethiols[67] and oligophenylenethiols[68]). The only deviation was the SAM formed from diSAc−OPE4 (2.47 μF cm^{-2}), which gave values nearly identical to those from diSAc−OPE3 (2.57 μF cm^{-2}). It is possible that this is the result of defects in the SAMs, which give higher values for capacitance, but unlikely given the close match between the predicted and measured values of thickness by ellipsometry. This same trend was observed in LAMJs (see below).

We measured the current-densities (J, A cm^{-2}) for the same series of SAMs in LAMJs at an applied bias of 0.5 V (Figure 9). These junctions comprise an evaporated Au bottom electrode, the SAM, a layer of PEDOT:PSS that serves as the top-contact, and a second evaporated Au electrode that is used to contact the PEDOT:PSS.[52] The measured values of J for OPE1−3 are averaged over hundreds of devices with diameters of 5−50 μm across two wafers for benzenedithiol and OPE2 and across three wafers for OPE3. When plotted on a logarithmic scale, these data are linear as a function of the thickness of the SAM. Using the equation $\ln J = J_0 - \beta d$ (where β is the characteristic decay, d is the length of the molecules in the SAM, and J_0 is the theoretical current-density at $d = 0$), we calculated β from the slope of OPE1−3 (Figure 9, blue ◆) to be 0.15 Å^{-1}. Typical values of β for thiol-terminated OPEs using STM break-junctions and CP-AFM are 0.34 and 0.21 Å^{-1}, respectively,[50,15] and are significantly lower than those found for alkanethiols (0.6−0.73 Å^{-1} in LAMJs[5,52] up to 0.9 Å^{-1} in many other junctions[48]). It is

cumbersome to make a direct comparison to these β values because of the different areas (single-molecule for STM, hundreds of molecules for CP-AFM, and areas of several micrometers for LAMJs) and contact geometries. However, 0.15 Å^{-1} is in good agreement with the value obtained for oligophenylenes in LAMJs (0.26 Å^{-1})[69] and in accordance with theoretical predictions (0.19 Å^{-1} for OPEs and 0.24−0.33 Å^{-1} for oligophenylenes).[70] For OPE4, we found a value very close to that of OPE3 (log J = 2.33 ± 0.29 A cm^{-2} for OPE4 (one wafer) vs 2.40 ± 0.50 A cm^{-2} for OPE3), a trend also observed in the capacitance measurements. The relatively high J of the SAMs of OPE4 might indicate the presence of defects in the SAMs of OPE4 (inconsistent with the data obtained by ellipsometry). Lu et al. observed a similar decrease in length dependence for a diamine series of OPE1−7.[71] They attribute this observation to a transition in the charge transport mechanism from tunneling to a hopping between OPE3 and OPE4.

To demonstrate the intimate connection between the mechanism of deprotection and the performance of ME devices, we measured J values of SAMs of diSAc−OPE3 without base (0.5 mM in THF, immersed for 2 days) and with 4 equiv of Bu$_4$NOH (0.3 mM in THF, immersed for 1 h). These data are summarized in Figure 9, red ●. For the SAMs without base, we found a J that was a factor 10 higher, which, in accordance with the lower apparent ellipsometric thickness, we attributed to a less densely packed SAM. The SAMs formed using Bu$_4$NOH resulted in devices with J values that were 2 orders of magnitude lower than that of the SAMs grown with Et$_3$N. This is due to either the formation of multilayers, the presence of Bu$_4$N$^+$, or the adsorption of polymerized disulfides on top of the SAM. Although we do not know the exact structure of this layer, these electrical measurements demonstrate that 4 equiv of Bu$_4$NOH gives SAMs of low quality. We note that in these experiments, despite the poor quality of the SAMs formed without base and using Bu$_4$NOH, we obtained functional (i.e., nonshorted) devices that produced reasonable values of J, highlighting the importance of using rigorously defined procedures to form SAMs for electrical measurements. Although it is common to assume that high-quality, densely packed SAMs form simply by treating a diSAc molecule with any base, we show that it is not valid to conclude that a SAM is of high quality simply from the observation of "reasonable" data in a ME device.

■ CONCLUSIONS

We draw two important conclusions from this work: (i) densely packed SAMs of linear, conjugated dithiols only form from solutions that contain primarily monothiolate and dithioacetate, but essentially no dithiolate, and (ii) the observation of reasonable data in ME devices is not sufficient evidence to conclude that a SAM is densely packed or of high quality. The only way to achieve a solution of monothiolate from diSAc molecules is to treat them with a base that forms monothiolate in sufficiently low quantities that the effective concentration of dithiolate in the solution is zero. We demonstrate unambiguously that this can be done using 9−15% Et$_3$N in THF and allowing (the high quality) SAM to form over 24−48 h. Dense SAMs will also form with 1 or 2 equiv of Bu$_4$NOH, but, after more than 2 h of immersion, multilayers will form. The use of any amount of Bu$_4$NOH will lead to the incorporation of some Bu$_4$N$^+$ in the monolayer, and too much Bu$_4$NOH will drive the equilibrium to the dithiolate, resulting in monolayers that are not upright

oriented SAMs, but chemisorbed molecules lying flat on the surface. For some ME measurements, it is not desirable to have a dense monolayer. In these cases, diSAc molecules can be used without deprotection to form reproducible, but not densely packed SAMs with thioacetate head groups. With this new understanding of the formation of SAMs, we can exert some control over the headgroup, which opens possibilities for new methods of contacting SAMs. It is our hope that the use of these procedures will eliminate the quality of the SAM as a variable in future work in ME.

■ ASSOCIATED CONTENT

ⓈSupporting Information. Reaction mechanisms and the results of additional UV−vis spectroscopy, ^{1}H NMR, ellipsometry, and electrochemical measurements; and the syntheses of SAc−OPE2 and SAc−OPE3. This material is available free of charge via the Internet at http://pubs.acs.org.

■ AUTHOR INFORMATION

Corresponding Author
r.c.chiechi@rug.nl; j.c.hummelen@rug.nl

Present Addresses
‖Center for Electron Transport in Molecular Nanostructures, Columbia University, 500 W 120th St., New York, NY 10027.

■ ACKNOWLEDGMENT

■ REFERENCES

(1) Carter, F. L. *J. Vac. Sci. Technol., B* **1983**, *1*, 959–968.
(2) Weibel, N.; Grunder, S.; Mayor, M. *Org. Biomol. Chem.* **2007**, *5*, 2343–2353.
(3) McCreery, R. L.; Bergren, A. J. *Adv. Mater.* **2009**, *21*, 4303–4322.
(4) van der Molen, S. J.; Liljeroth, P. *J. Phys.: Condens. Matter* **2010**, *22*, 133001.
(5) Akkerman, H. B.; Blom, P. W. M.; de Leeuw, D. M.; de Boer, B. *Nature* **2006**, *441*, 69–72.
(6) Love, J. C.; Estroff, L. A.; Kriebel, J. K.; Nuzzo, R. G.; Whitesides, G. M. *Chem. Rev.* **2005**, *105*, 1103–1169.
(7) Tour, J. M.; Jones, L. R., II; Pearson, D. L.; Lamba, J. J. S.; Burgin, T. P.; Whitesides, G. M.; Allara, D. L.; Parikh, A. N.; Atre, S. V. *J. Am. Chem. Soc.* **1995**, *117*, 9529–9534.
(8) Azzam, W.; Wehner, B. I.; Fischer, R. A.; Terfort, A.; Wöll, C. *Langmuir* **2002**, *18*, 7766–7769.
(9) Seferos, D. S.; Banach, D. A.; Alcantar, N. A.; Israelachvili, J. N.; Bazan, G. C. *J. Org. Chem.* **2004**, *69*, 1110–1119.
(10) In contrast to the results in refs 7 and 9, the formation of SAMs from diSAc−OPE3 without deprotection was reported to give the expected thickness: Lau, K. H. A.; Huang, C.; Yakovlev, N.; Chen, Z. K.; O'Shea, S. J. *Langmuir* **2006**, *22*, 2968–2971.
(11) de Boer, B.; Meng, H.; Perepichka, D. F.; Zheng, J.; Frank, M. M.; Chabal, Y. J.; Bao, Z. *Langmuir* **2003**, *19*, 4272–4284.
(12) Walzer, K.; Marx, E.; Greenham, N. C.; Less, R. J.; Raithby, P. R.; Stokbro, K. *J. Am. Chem. Soc.* **2004**, *126*, 1229–1234.
(13) Maya, F.; Flatt, A. K.; Stewart, M. P.; Shen, D. E.; Tour, J. M. *Chem. Mater.* **2004**, *16*, 2987–2997.
(14) Kronemeijer, A. J.; Akkerman, H. B.; Kudernac, T.; Wees, B. J.; Feringa, B. L.; Blom, P. W. M.; de Boer, B. *Adv. Mater.* **2008**, *20*, 1467–1473.
(15) Liu, K.; Li, G.; Wang, X.; Wang, F. *J. Phys. Chem. C* **2008**, *112*, 4342–4349.
(16) Shaporenko, A.; Elbing, M.; Blaszczyk, A.; von Hänisch, C.; Mayor, M.; Zharnikov, M. *J. Phys. Chem. B* **2006**, *110*, 4307–4317.
(17) Colavita, P. E.; Miney, P. G.; Taylor, L.; Priore, R.; Pearson, D. L.; Ratliff, J.; Ma, S.; Ozturk, O.; Chen, D. A.; Myrick, M. L. *Langmuir* **2005**, *21*, 12268–12277.
(18) Zeng, X.; Wang, C.; Batsanov, A. S.; Bryce, M. R.; Gigon, J.; Urasinska-Wojcik, B.; Ashwell, G. J. *J. Org. Chem.* **2010**, *75*, 130–136.
(19) Cheng, L.; Yang, J.; Yao, Y.; Price, D. W., Jr.; Dirk, S. M.; Tour, J. M. *Langmuir* **2004**, *20*, 1335–1341.
(20) Berner, S.; Lidbaum, H.; Ledung, G.; Åhlund, J.; Nilson, K.; Schiessling, J.; Gelius, U.; Bäckvall, J.; Puglia, C.; Oscarsson, S. *Appl. Surf. Sci.* **2007**, *253*, 7540–7548.
(21) Ponticello, G. S.; Habecker, C. N.; Varga, S. L.; Pitzenberger, S. M. *J. Org. Chem.* **1989**, *54*, 3223–3224.
(22) Yu, C.; Chong, Y.; Kayyem, J.; Gozin, M. *J. Org. Chem.* **1999**, *64*, 2070–2079.
(23) Elbing, M.; Blaszczyk, A.; Hänisch, C. V.; Mayor, M.; Ferri, V.; Grave, C.; Rampi, M. A.; Pace, G.; Samor, P.; Shaporenko, A.; Zharnikov, M. *Adv. Funct. Mater.* **2008**, *18*, 2972–2983.
(24) Cai, L.; Yao, Y.; Yang, J.; Price, D. W., Jr.; Tour, J. M. *Chem. Mater.* **2002**, *14*, 2905–2909.
(25) Stapleton, J. J.; Harder, P.; Daniel, T. A.; Reinard, M. D.; Yao, Y.; Price, D. W.; Tour, J. M.; Allara, D. L. *Langmuir* **2003**, *19*, 8245–8255.
(26) Hacker, C. A.; Batteas, J. D.; Garno, J. C.; Marquez, M.; Richter, C. A.; Richter, L. J.; van Zee, R. D.; Zangmeister, C. D. *Langmuir* **2004**, *20*, 6195–6205.
(27) Grunder, S.; Huber, R.; Horhoiu, V.; González, M. T.; Schönenberger, C.; Calame, M.; Mayor, M. *J. Org. Chem.* **2007**, *72*, 8337–8344.
(28) Huber, R.; Gonzalez, M. T.; Wu, S.; Langer, M.; Grunder, S.; Horhoiu, V.; Mayor, M.; Bryce, M.; Wang, C.; Jitchati, R.; Schönenberger, C.; Calame, M. *J. Am. Chem. Soc.* **2008**, *130*, 1080–1084.
(29) Wu, S.; González, M. T.; Huber, R.; Grunder, S.; Mayor, M.; Schönenberger, C.; Calame, M. *Nat. Nanotechnol.* **2008**, *3*, 569–574.
(30) Grunder, S.; Huber, R.; Wu, S.; Schönenberger, C.; Calame, M.; Mayor, M. *Eur. J. Org. Chem.* **2010**, *2010*, 833–845.
(31) Mishchenko, A.; Vonlanthen, D.; Meded, V.; Bürkle, M.; Li, C.; Pobelov, I. V.; Bagrets, A.; Viljas, J. K.; Pauly, F.; Evers, F.; Mayor, M.; Wandlowski, T. *Nano Lett.* **2010**, *10*, 156–163.
(32) Xia, Y.; Whitesides, G. M. *Angew. Chem., Int. Ed.* **1998**, *37*, 550–575.
(33) Loo, Y.; Lang, D. V.; Rogers, J. A.; Hsu, J. W. P. *Nano Lett.* **2003**, *3*, 913–917.
(34) Niskala, J. R.; You, W. *J. Am. Chem. Soc.* **2009**, *131*, 13202–13203.
(35) Milani, F.; Grave, C.; Ferri, V.; Samor, P.; Rampi, M. A. *ChemPhysChem* **2007**, *8*, 515–518.
(36) Slowinski, K.; Fong, H. K. Y.; Majda, M. *J. Am. Chem. Soc.* **1999**, *121*, 7257–7261.
(37) York, R. L.; Nguyen, P. T.; Slowinski, K. *J. Am. Chem. Soc.* **2003**, *125*, 5948–5953.
(38) Weiss, E. A.; Chiechi, R. C.; Kaufman, G. K.; Kriebel, J. K.; Li, Z.; Duati, M.; Rampi, M. A.; Whitesides, G. M. *J. Am. Chem. Soc.* **2007**, *129*, 4336–4349.
(39) Chiechi, R. C.; Weiss, E. A.; Dickey, M. D.; Whitesides, G. M. *Angew. Chem., Int. Ed.* **2008**, *47*, 142–144.

(40) Nijhuis, C. A.; Reus, W. F.; Whitesides, G. M. *J. Am. Chem. Soc.* **2009**, *131*, 17814–17827.

(41) Wold, D. J.; Frisbie, C. D. *J. Am. Chem. Soc.* **2001**, *123*, 5549–5556.

(42) Engelkes, V. B.; Beebe, J. M.; Frisbie, C. D. *J. Phys. Chem. B* **2005**, *109*, 16801–16810.

(43) Choi, S. H.; Risko, C.; Delgado, M. C. R.; Kim, B.; Brédas, J.; Frisbie, C. D. *J. Am. Chem. Soc.* **2010**, *132*, 4358–4368.

(44) Scaini, D.; Castronovo, M.; Casalis, L.; Scoles, G. *ACS Nano* **2008**, *2*, 507–515.

(45) Mantooth, B. A.; Weiss, P. S. *Proc. IEEE* **2003**, *9*, 1785–1802.

(46) Salomon, A.; Cahen, D.; Lindsay, S.; Tomfohr, J.; Engelkes, V. B.; Frisbie, C. D. *Adv. Mater.* **2003**, *15*, 1881–1890.

(47) Haick, H.; Cahen, D. *Prog. Surf. Sci.* **2008**, *83*, 217–261.

(48) Akkerman, H. B.; de Boer, B. *J. Phys.: Condens. Matter* **2008**, *20*, 013001.

(49) Stuhr-Hansen, N.; Sørensen, J. K.; Moth-Poulsen, K.; Christensen, J. B.; Bjørnholm, T.; Nielsen, M. B. *Tetrahedron* **2005**, *61*, 12288–12295.

(50) Kaliginedi, V.; Valkenier, H.; García-Suárez, V. M.; Moreno-García, P.; Hong, W.; Buiter, P.; Otten, J. L. H.; Hummelen, J. C.; Lambert, C.; Wandlowski, Th., manuscript in preparation.

(51) WinSpec 2.09, developed at Laboratoire Interdépartemental de Spectroscopie Electronique, Namur, Belgium.

(52) van Hal, P. A.; Smits, E. C. P.; Geuns, T. C. T.; Akkerman, H. B.; de Brito, B. C.; Perissinotto, S.; Lanzani, G.; Kronemeijer, A. J.; Geskin, V.; Cornil, J.; Blom, P. W. M.; de Boer, B.; de Leeuw, D. M. *Nat. Nanotechnol.* **2008**, *3*, 749–754.

(53) Um, I.; Lee, J.; Bae, S.; Buncel, E. *Can. J. Chem.* **2005**, *83*, 1365–1371.

(54) Wallace, O. B.; Springer, D. M. *Tetrahedron Lett.* **1998**, *39*, 2693–2694.

(55) Schreiber, F. *Prog. Surf. Sci.* **2000**, *65*, 151–256.

(56) Impurities in the monolayer are the result of molecules becoming kinetically trapped, which can occur in either phase; that is, an impurity can be incorporated into the growing islands or interrupt the growth of an island by lying down. These impurities can be other molecules (e.g., S—Ar in a SAM of SAc—Ar—S) or molecules that are not incorporated correctly (e.g., upside-down).

(57) SAc—OPE—SH molecules have been synthesized, but the mechanism is the same as SAc—OPE—SAc except that SH is cleaved faster than SAc by Au and is probably better in filling the defects of the SAM, see: (a) Flatt, A. K.; Yao, Y.; Maya, F.; Tour, J. M. *J. Org. Chem.* **2004**, *69*, 1752–1755. (b) Niklewski, A.; Azzam, W.; Strunskus, T.; Fischer, R. A.; Wöll, C. *Langmuir* **2004**, *20*, 8620–8624. See the Supporting Information for a more detailed discussion on thiols.

(58) Although the resolution of this spectrum is low, we confirmed these assignments with a higher resolution spectrum; see Figure S8.

(59) diS—OPE3 is probably present in the solution, however, in quantities below the detection limit of ^{1}H NMR (~5%).

(60) The S—S distance of diS—OPE3 is 19.8 Å, corresponding to a maximum theoretical thickness of 24.9 Å for a SAM of AuS—OPE3—SAc and 22.1 Å for a SAM of AuS—OPE3—S.

(61) Krapchetov, D. A.; Ma, H.; Jen, A. K. Y.; Fischer, D. A.; Loo, Y. *Langmuir* **2005**, *21*, 5887–5893. Krapchetov, D. A.; Ma, H.; Jen, A. K. Y.; Fischer, D. A.; Loo, Y. *Langmuir* **2006**, *22*, 9491–9494. Krapchetov, D. A.; Ma, H.; Jen, A. K. Y.; Fischer, D. A.; Loo, Y. *Langmuir* **2008**, *24*, 851–856.

(62) In two other studies from the same group, acetyl esters of monothiols are deprotected with Et$_3$N: (a) Shaporenko, A.; Rössler, K.; Lang, H.; Zharnikov, M. *J. Phys. Chem. B* **2006**, *110*, 24621–24628. (b) Weidner, T.; Rössler, K.; Ecorchard, P.; Lang, H.; Grunze, M.; Zharnikov, M. *J. Electroanal. Chem.* **2008**, *621*, 159–170.

(63) Precipitate was formed in the solution of diSAc—OPE4 over time. To prevent this precipitate from contaminating the SAM, the samples were placed upside-down in solution (see Figure S10).

(64) Sauer, J. C. *J. Am. Chem. Soc.* **1947**, *69*, 2444–2448.

(65) Wedekind, E. *Ber. Dtsch. Chem. Ges.* **1901**, *34*, 2070–2077.

(66) No Et$_3$N was added to the solution of benzenedithiol in THF.

(67) Porter, M. D.; Bright, T. B.; Allara, D. L.; Chidsey, C. E. D. *J. Am. Chem. Soc.* **1987**, *109*, 3559–3568.

(68) Sabatani, E.; Cohen-Boulakia, J.; Bruening, M.; Rubinstein, I. *Langmuir* **1993**, *9*, 2974–2981.

(69) Kronemeijer, A. J.; Huisman, E. H.; Akkerman, H. B.; Goossens, A. M.; Katsouras, I.; van Hal, P. A.; Geuns, T. C. T.; van der Molen, S. J.; Blom, P. W. M.; de Leeuw, D. M. *Appl. Phys. Lett.* **2010**, *97*, 173302. The β value of 0.26 Å^{-1} found for oligophenyelenes in LAMJs is smaller than those reported for other geometries.

(70) Liu, H.; Wang, N.; Zhao, J.; Guo, Y.; Yin, X.; Boey, F. Y. C.; Zhang, H. *ChemPhysChem* **2008**, *9*, 1416–1424.

(71) Lu, Q.; Liu, K.; Zhang, H.; Du, Z.; Wang, X.; Wang, F. *ACS Nano* **2009**, *3*, 3861–3868.